Hindawi
Discrete Dynamics in Nature and Society
Volume 2018, Article ID 6946492, 9 pages
https://doi.org/10.1155/2018/6946492

Research Article

Deformation Analysis of Reinforced Retaining Wall Using Separate Finite Element

Xingli Jia[1], **Jinliang Xu**[1] **and Yuhai Sun**[2]

[1]*School of Highway, Chang'an University, Xi'an 710064, China*
[2]*Shandong Provincial Communications Planning and Design Institute, Jinan 250031, China*

Correspondence should be addressed to Xingli Jia; jxl0126@sina.com

Received 18 December 2017; Accepted 5 July 2018; Published 5 September 2018

Academic Editor: Alicia Cordero

In order to reveal the main factors affecting the deformation of reinforced soil retaining wall and the influence of various factors on the deformation, the constitutive relation is discretized into four aspects of soil, geogrid, wall panel, and contact surface, and discrete element matrices are, respectively, constructed, with the method of separate finite element. Based on the finite element geotechnical analysis technology platform, the deformation analysis model of reinforced soil retaining wall is established. Taking the modulus of foundation soil as the influencing factor of the foundation soil, taking the geogrid stiffness, length, and spacing as the influencing factors of geogrids, and taking the filling type of limestone, fly ash, and silty clay as the influencing factors of backfill in the wall, the horizontal and vertical deformations of reinforced retaining wall under different factors using the methods of controlling a single variable analysis are calculated. The results show that the increase of elastic modulus of foundation soil will reduce the vertical deformation of the wall but increase the horizontal deformation. The silty clay is not suitable as filler, and lime soil is slightly better than fly ash. The spacing between geogrids is 20 cm ~ 60 cm, which has less effect on wall deformation, but the horizontal deformation rapidly increases after the spacing increases to 80 cm, and other grid performance influencing factors also have the characteristic, where there exists a threshold. The wall will have a greater deformation when the threshold is not reached; a higher indicator of the grid to reduce the deformation of the retaining wall is not obvious after reaching the threshold.

1. Introduction

As a typical flexible retaining structure, reinforced soil retaining wall has the characteristics of beautiful appearance, less occupation, good coordination, convenient construction, and strong adaptability [1, 2] and can improve the strength and stability of roadbed, is widely used in highway infrastructure construction, and has become an important part of highway infrastructure construction. However, due to the complicated engineering characteristics of the reinforced soil retaining wall itself, the nonlinear changes of various factors in different conditions, and the interaction between various factors, the deformation characteristics of the reinforced retaining wall are relatively complex.

The deformation of the reinforced retaining wall is affected by many factors, not only its wall structure and filling material, but also the properties of the reinforced material [3]. The deformation data of reinforced soil retaining wall can be observed by field observation, which is true and accurate [4], while lacking general applicability because of the variety of environment, construction technology, and operating status with strong individual differences.

Large-scale finite element simulation technology is introduced into the deformation analysis of reinforced earth retaining wall to reduce the analysis error caused by individual heterogeneity. The stress-strain characteristics and the interaction between soil effects [5, 6] of the material can be considered with the using of finite element method, to accurately simulate deformation trend of the wall. Clough [7] reviewed and derived the finite element incremental formulations for nonlinear static and dynamic analysis, including large displacements, large strains, and material nonlinearities, and the solution of static and dynamic problems involving large displacements and large strains are presented. Zhang [8] analyzed geogrid deformation, wall bottom pressure, and fracture plane of the retaining wall according to the field

test on three different geogrid reinforced earth high retaining walls. The results show that there is a single peak in the pressure distribution at the bottom of the wall. Chen [9] gave out finite element modeling, which were performed on RSW with various fillings and foundations. The results indicate that a statistical function relationship exhibits between the maximum settlement and the facing slope at the bottom of RSW. Anastasopoulos [10] studied the seismic performance of a typical bar-mat retaining wall theoretically and experimentally, a series of reduced-scale shaking table tests are carried out with various kinds of earthquake excitation (real records and artificial multicycle motions), and the problem is carried out by finite element method. Mowafy [11] states that deformation caused by wall movement is an important indicator of reinforced earth retaining wall; the influence of reinforcement global stiffness, the height of the wall, the friction angle of the soil on the earth pressure coefficient, and the maximum wall displacement are important with the using of the finite element program, ANSYS. Yang [12] built finite element models that are used to simulate the behavior of large-scale geosynthetic reinforced soil retaining walls, showing that the constitutive models and finite element model can predict the important features of wall performance accurately. Ye [13] conducted a finite element analysis to simulate a reinforced earth retaining wall for embankment by using the finite element software Plaxis; the calculated results of reinforced earth retaining wall with three facing types are analyzed, including the lateral earth pressure and the vertical earth pressure, to investigate the influence of different facing types on the mechanical properties of the reinforced earth retaining wall for embankment. Bui [14] simulated postfailure behavior and large deformations of soils and retaining wall blocks in SRW systems, using a new computational framework based on smooth particle hydrodynamics (SPH) method, within which a new contact model is proposed to simulate the interaction between the soil and the blocks and between the blocks. Ouria [15] established the finite element model which is used to study the behavior of a CFRP reinforced wall based on the laboratory results for backfill soil and interface data. Ou [16] analyzed the retaining wall vertical deformation impact parameters such as reinforced spacing, foundation stiffness, and lateral deformation by using the nonlinear analysis software ADINA. The results indicate that rational design of grid, panel, foundation, cushion modulus, and thickness can effectively lessen the vertical deformation and uneven settlement of the retaining wall. Wu [17] used the analysis focused on the dynamic response characteristics of the wall under the influence of different reinforcement to study the dynamic properties of reinforced earth retaining walls under seismic load which were analyzed by using Plaxis.

The typical filling type, reinforced material, and wall structure are selected, and the constitutive relation and element matrix are constructed by using the separated finite element method, to find out the general rule of the deformation of reinforced soil retaining wall. The influence mode and degree of various factors on the deformation of reinforced earth retaining wall are analyzed, and the technical reference for improving the stability of the wall is finally provided.

2. Theory and Method

2.1. Constitutive Relation Model. The deformation of soil is determined by soil plasticity, and the basis of determining whether the soil makes plastic deformation is the yield function, reflecting the relationship between stress and strain of soil; soil constitutive relationship is the stress-strain relationship; the Molar Coulomb elastoplastic model (Mohr-Coulomb) is used in this study [18, 19]. The study of reinforcement materials is geogrid, which is a material of higher strength and modulus, buried and pulled in the filler layer by layer, the geogrid is identified as a one-dimensional linear rod unit that is subjected only to tension without stress and capable of axial strain only. Wall panels are made of concrete blocks, wall panels can be simplified as a plate model, and the linear elastic constitutive relations are used in geogrid and wall panels. Discrete analysis is used to separate the reinforced material from the soil, and there is a relative displacement between the two. The contact surface unit is set up between the two. The frictional resistance is generated during the relative movement of the reinforced material and the soil.

2.2. Finite Element Matrix. The study is to solve the problem of plane strain, using the displacement method. The element matrix of each element of soil, geogrid, wall panel, and contact surface should be deduced, respectively, and the stress, strain, and displacement should be solved according to the corresponding matrix [20].

2.2.1. Soil Element Matrix. The soil unit selects the triangular element body, and the displacement at the node is expressed as

$$\{\delta\}^e = \{u_i \;\; v_i \;\; u_j \;\; v_j \;\; u_m \;\; v_m\}^T \tag{1}$$

The displacement at any place in the unit is expressed as

$$\{\delta(x,y)\} = \begin{Bmatrix} u(x,y) \\ v(x,y) \end{Bmatrix} = \begin{Bmatrix} \alpha_1 + \alpha_2 x + \alpha_3 y \\ \alpha_4 + \alpha_5 x + \alpha_6 y \end{Bmatrix} \tag{2}$$

The displacement at the node is expressed as

$$\begin{Bmatrix} u_i \\ u_j \\ u_m \end{Bmatrix} = \begin{bmatrix} 1 & x_i & y_i \\ 1 & x_j & y_j \\ 1 & x_m & y_m \end{bmatrix} \begin{Bmatrix} a_1 \\ a_2 \\ a_3 \end{Bmatrix}$$
$$\begin{Bmatrix} v_i \\ v_j \\ v_m \end{Bmatrix} = \begin{bmatrix} 1 & x_i & y_i \\ 1 & x_j & y_j \\ 1 & x_m & y_m \end{bmatrix} \begin{Bmatrix} a_4 \\ a_5 \\ a_6 \end{Bmatrix} \tag{3}$$

Let

$$A = \begin{bmatrix} 1 & x_i & y_i \\ 1 & x_j & y_j \\ 1 & x_m & y_m \end{bmatrix},$$
$$\Delta = \frac{1}{2}\begin{vmatrix} 1 & x_i & y_i \\ 1 & x_j & y_j \\ 1 & x_m & y_m \end{vmatrix} \tag{4}$$

It can be obtained that

$$\begin{Bmatrix} a_1 \\ a_2 \\ a_3 \end{Bmatrix} = \frac{1}{2\Delta}\begin{bmatrix} a_i & a_j & a_m \\ b_i & b_j & b_m \\ c_i & c_j & c_m \end{bmatrix}\begin{Bmatrix} u_i \\ u_j \\ u_m \end{Bmatrix},$$
$$\begin{Bmatrix} a_4 \\ a_5 \\ a_6 \end{Bmatrix} = \frac{1}{2\Delta}\begin{bmatrix} a_i & a_j & a_m \\ b_i & b_j & b_m \\ c_i & c_j & c_m \end{bmatrix}\begin{Bmatrix} v_i \\ v_j \\ v_m \end{Bmatrix} \tag{5}$$

$$a_i = x_j y_m - x_m y_j,$$
$$b_i = y_j - y_m, \tag{6}$$
$$c_i = x_m - x_j$$

The shape function selected is expressed as

$$N_i = \frac{a_i + b_i x + c_i y}{2\Delta},$$
$$N_j = \frac{a_j + b_j x + c_j y}{2\Delta}, \tag{7}$$
$$N_m = \frac{a_m + b_m x + c_m y}{2\Delta}$$

The element stiffness matrix is expressed as

$$[K]^e = [B]^T \cdot [D] \cdot [B] \cdot A \cdot t \tag{8}$$

According to the principle of virtual work

$$\{F\}^e = [K]^e \cdot \{\delta\}^e \tag{9}$$

$\{\delta\}^e$ is solved:

$$\{\delta(x, y)\} = \begin{bmatrix} N_i & 0 & N_j & 0 & N_m & 0 \\ 0 & N_i & 0 & N_j & 0 & N_m \end{bmatrix}\{\delta\}^e \tag{10}$$

$$\{\varepsilon\} = [B] \cdot \{\delta\}^e \tag{11}$$

$$\{\sigma\} = [D] \cdot \{\varepsilon\}^e = [D] \cdot [B] \cdot \{\delta\}^e = [S] \cdot \{\delta\}^e \tag{12}$$

where $\{\delta\}^e$ is the displacement at the node, $\{\delta(x, y)\}$ is the displacement at any place in the unit, $\{\sigma\}$ is the stress at any place in the unit, $\{\varepsilon\}$ is the strain at any place in the unit, $[K]^e$ is the stiffness matrix of the unit, $[B]$ is the strain matrix of the unit, $[D]$ is the elastic matrix of the unit, and $[S]$ is the stress matrix of the unit, t is the thickness of the unit, the general value is 1.

2.2.2. Geogrid Element Matrix. The constitutive relation of the geogrid element is linear elastic [21], and its stiffness matrix is defined as

$$[K]^{\varepsilon} = \frac{E_n W}{L\begin{Bmatrix} c^2 & cs & -c^2 & -cs \\ cs & s^2 & cs & -s^2 \\ -c^2 & cs & c^2 & cs \\ -cs & -s^2 & cs & s^2 \end{Bmatrix}} \tag{13}$$

E_n is the elastic modulus of geogrid (KN/m^2); W is the equivalent section area (m^2); L is the length of the geogrid (m).

$s = \sin\alpha$, $c = \cos\alpha$, α is the angle between the geogrid unit and the X axis of the coordinate system.

The calculation methods of node force, node displacement, stress, strain, and deformation are the same.

2.2.3. Wall Panel Element Matrix. The constitutive relation of the wall panel element is linear elastic, and its stiffness matrix is defined as

$$[K]^e = \frac{EI}{l^3}\begin{Bmatrix} 12 & 6l & -12 & 6l \\ 6l & 4l^2 & -6l & 2l^2 \\ -12 & -6l & 12 & -6l \\ 6l & 2l^2 & -6l & 4l^2 \end{Bmatrix} \tag{14}$$

E is the elastic modulus of the beam element of the wall panel; I is the inertia moment of a section on a unit length; l is unit length.

The element stiffness matrix above is established in natural coordinates, while the natural coordinates are not consistent with the overall coordinates in some cases that the conversion between the two coordinate systems needs to be performed, which is not described in detail herein.

The calculation methods of node force, node displacement, stress, strain, and deformation are the same.

2.2.4. Contact Surface Element Matrix. The contact surface model is made up of four-node element matrix without thickness, which is composed of two contact surfaces 12 and 34 with a length of L, assuming that there are numerous microsprings between the two interfaces to connect. The 12 and 34 contact surfaces are connected in one block and can be regarded as a one-dimensional unit, before subjected to force [22]. The relationship between the soil element and the contact surface unit and the geogrid unit will be related to the relevant forces only at the junction. Assuming that the displacement mode is linear, the displacement of the node can be expressed as the displacement of each point in the direction of the contact surface along the length direction. The displacement in the direction of X coordinates is expressed by u, and the displacement in the direction of the Y coordinates is expressed by v.

The displacement of the top surface is as follows:

$$\begin{Bmatrix} u_{top} \\ v_{top} \end{Bmatrix} = \frac{1}{2} \begin{bmatrix} 1+\frac{2x}{L} & 0 & 1-\frac{2x}{L} & 0 \\ 0 & 1+\frac{2x}{L} & 0 & 1-\frac{2x}{L} \end{bmatrix} \begin{Bmatrix} u_3 \\ v_3 \\ u_4 \\ v_4 \end{Bmatrix} \quad (15)$$

The displacement of the bottom is as follows:

$$\begin{Bmatrix} u_{bottom} \\ v_{bottom} \end{Bmatrix} = \frac{1}{2} \begin{bmatrix} 1-\frac{2x}{L} & 0 & 1+\frac{2x}{L} & 0 \\ 0 & 1-\frac{2x}{L} & 0 & 1+\frac{2x}{L} \end{bmatrix} \begin{Bmatrix} u_1 \\ v_1 \\ u_2 \\ v_2 \end{Bmatrix} \quad (16)$$

The displacement of any point on the unit body of the contact surface can be interpolated by the node displacement, as follows:

$$\begin{aligned} \{w\} &= \begin{Bmatrix} w_s \\ w_n \end{Bmatrix} = \begin{Bmatrix} u_{bottom} - u_{top} \\ v_{bottom} - v_{top} \end{Bmatrix} \\ &= \begin{bmatrix} a & 0 & b & 0 & -b & 0 & -a & 0 \\ 0 & a & 0 & b & 0 & -b & 0 & -a \end{bmatrix} \{\delta\}^e \\ \{\delta\}^e &= \begin{bmatrix} u_1 & v_1 & u_2 & v_2 & u_3 & v_3 & u_4 & v_4 \end{bmatrix}^T \end{aligned} \quad (17)$$

where

$$\begin{aligned} a &= \frac{1}{2} - \frac{X}{L} \\ b &= \frac{1}{2} + \frac{X}{L} \end{aligned} \quad (18)$$

Let

$$[B] = \begin{bmatrix} a & 0 & b & 0 & -b & 0 & -a & 0 \\ 0 & a & 0 & b & 0 & -b & 0 & -a \end{bmatrix} \quad (19)$$

Get

$$\{w\} = [B] \bullet \{\delta\}^e \quad (20)$$

According to the principle of virtual displacement, it can be obtained:

$$\{F\}^e = [K] \bullet \{\delta\}^e \quad (21)$$

The node displacement will be obtained by superimposing the stiffness matrix of each contact element on the global stiffness matrix; through the general balance condition of nodes, the stress and deformation are then obtained according to $\{w\} = [B] \bullet \{\delta\}^e$, $\{\sigma\} = [K] \bullet \{w\}$.

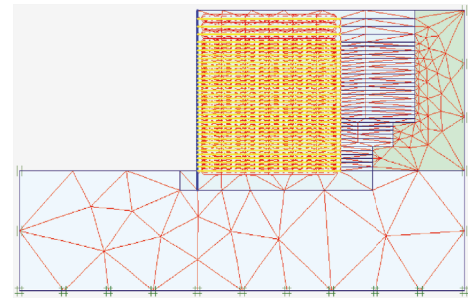

Figure 1: finite element mesh model.

2.3. Deformation Analysis Model Based on the Separated Finite Element. The Plaxis is used to establish the finite element stability analysis model of the reinforced soil retaining wall. The interface unit is introduced in the modeling, which mainly includes the horizontal interface between the reinforced material and the filler, and the vertical interface between the wall panel and the filler. The triangular element of fifteen nodes is used in the division of the finite element meshes; the standard fixed boundary is selected. The materials used, such as geogrids, packing, foundation soil, and graded gravel, were taken from the site of the DeShang Expressway. The properties of the geogrid are shown in Table 1.

The finite element model is built on the basis of practical work. The length of the retaining wall in the project is 70 m, the precast concrete is used for the material of wall panel, the strength grade of the retaining wall is C30, the height of it is 8 m, the paving internal of the geogrid is 20 cm in the retaining wall, 40 cm on the top, and the length of the geogrid is 8 m. The total thickness of graded crushed stone in the foundation is 60 cm, which is divided into two layers, each layer is 30 cm, and the total length is 10.65 m. The finite element model of reinforced soil retaining wall in this paper is shown in Figure 1.

3. Results and Discussion

In order to study the influence of various factors on the wall deformation, the basic wall shape is token as the foundation, and the influence factors are studied through the method of controlling the single variable. The influencing factors of this study include the modulus of foundation soil, the stiffness and length of geogrid, the spacing between geogrids, the stiffness of wall panels, and the fill behind walls.

3.1. The Influence of Foundation Soil Modulus on the Deformation of Retaining Wall. The foundation soil with elastic modulus of 13Mpa, 20Mpa, 27Mpa, 34Mpa, and 41Mpa is calculated, respectively. The results of the horizontal deformation of the wall are shown in Figure 2, respectively.

It can be perceived that when the elastic modulus of the foundation soil reduces to 20Mpa and 13Mpa, the maximum horizontal deformation increases by 33% and 103%, respectively. It is obvious that the settlement and deformation of the foundation will increase with the increase of the elastic modulus of the foundation soil, and the horizontal

Table 1: The properties of the reinforced material.

Type	Axial stiffness (KN/m)	Tensile Strength (KN/m)	2% Tensile Strength (KN/m)	5% Tensile Strength (KN/m)	Nominal Elongation (%)	Introduction
TGDG80	800	≥80.0	≥21.0	≥40.0	≤10.0	Unidirectional geogrid

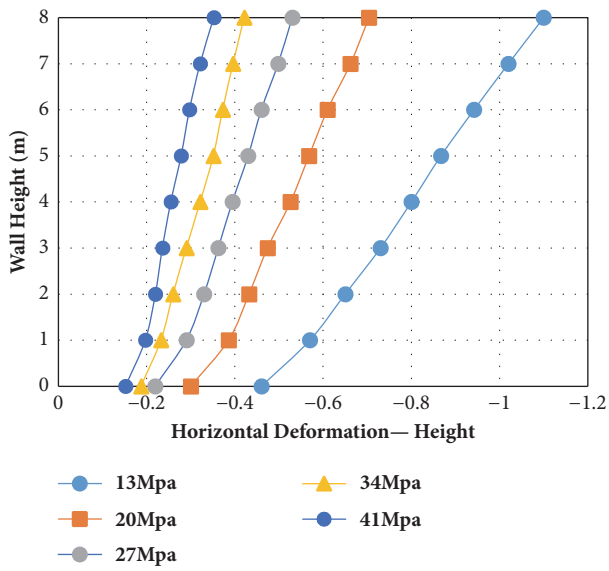

Figure 2: Effect of foundation soil on horizontal deformation of the wall.

deformation of the wall will also increase. At the same time, if the bearing capacity of the foundation is insufficient, the instability of the wall will be caused. On the contrary, when the elastic modulus of the foundation soil increases to 34Mpa and 41Mpa, the horizontal deformation decreases by 22% and 35%, respectively. It indicates that the greater the elastic modulus of the foundation soil, the smaller the effect of increasing the elastic modulus of the foundation soil will have on the horizontal deformation of the retaining wall.

The results of the vertical deformation of the wall are shown in Figure 3, respectively.

As can be seen from the Figure 3, the elastic modulus of foundation soil has a great influence on vertical deformation of the retaining wall, and the vertical deformation of wall decreases significantly when the modulus of elasticity of foundation soil increases. When the elastic modulus of the foundation soil is 41 Mpa, the maximum vertical deformation is only 2.7 mm, and it can run up to 7.5 mm when the elastic modulus of the foundation soil is 13 Mpa. The maximum displacement occurs near the vertical direction of the retaining wall, and the vertical displacement decreases from the wall to the inside. On the soft soil foundation, the vertical deformation decreases obviously faster than that on the foundation with large elastic modulus, which may lead to the uneven settlement of the wall. It can be concluded that the foundation must be treated when the elastic modulus of the foundation is too small.

3.2. The Influence of Geogrid Strength on the Deformation of Retaining Wall. The horizontal deformation of the geogrid is calculated by 100 kN/m, 300 kN/m, 500 kN/m, 800 kN/m, and 1000 kN/m, respectively. The results are shown in Figure 4.

It can be seen that from Figure 4 when the grid strength decreases from 300 kN/m to 100kn/m, the maximum horizontal deformation increases by 23%. When the grid strength continues to increase, the maximum horizontal deformation decreases, and the decrease range is reduced. In other words, when the geogrid intensity reaches a certain level, the horizontal deformation of the wall decreases and slows down. The geogrid strength of retaining wall has a certain effect on the vertical deformation which is not obvious, while having a certain effect on the wall near the outside. The influence of geogrid on vertical deformation of retaining wall mainly indirectly affects the settlement of the retaining wall by influencing horizontal deformation. In fact, the influence of various parameters of grille on retaining wall settlement is similar to that of grille, which indirectly affects the settlement of retaining wall by influencing horizontal deformation.

The same calculation method was used to select the geogrid spacing of 20 cm, 40 cm, 60 cm, and 80 cm and the geogrid length of 6 m, 7 m, 8 m, and 9 m for finite element analysis. The results are shown in Figure 5.

The results show that the deformation of the wall decreases with the shrinking of the spacing between the geogrids. When the spacing between geogrids is 20 cm~ 60 cm, the deformation of the wall is less affected, while when the spacing between geogrids increases to 80 cm, the horizontal deformation of the wall increases rapidly. It can be inferred that when the stiffened spacing is reduced to a certain extent under other conditions which remain unchanged, the effect of continuing to reduce the stiffened spacing on the horizontal deformation of the retaining wall is not obvious.

The growth of geogrid length has great influence on wall deformation when it increases from 6 m to 7 m, while having little effect on the wall when the length is over 7 m. That is to say, there is a limit value for the reinforcement length under a certain height of the retaining wall. When the length of the geogrid exceeds the limit value, the extra length of the geogrid will not work too much. It can be considered that the increase of the length of the geogrid does not necessarily improve the deformation of the wall.

The influence of the geogrid on the retaining wall has a more obvious characteristics, where there exists a threshold. A large deformation on the wall will occur when an index is not up to the requirements of the grid, while not obvious after the threshold is reached. The grid has a certain influence on the vertical deformation of the retaining wall, which is

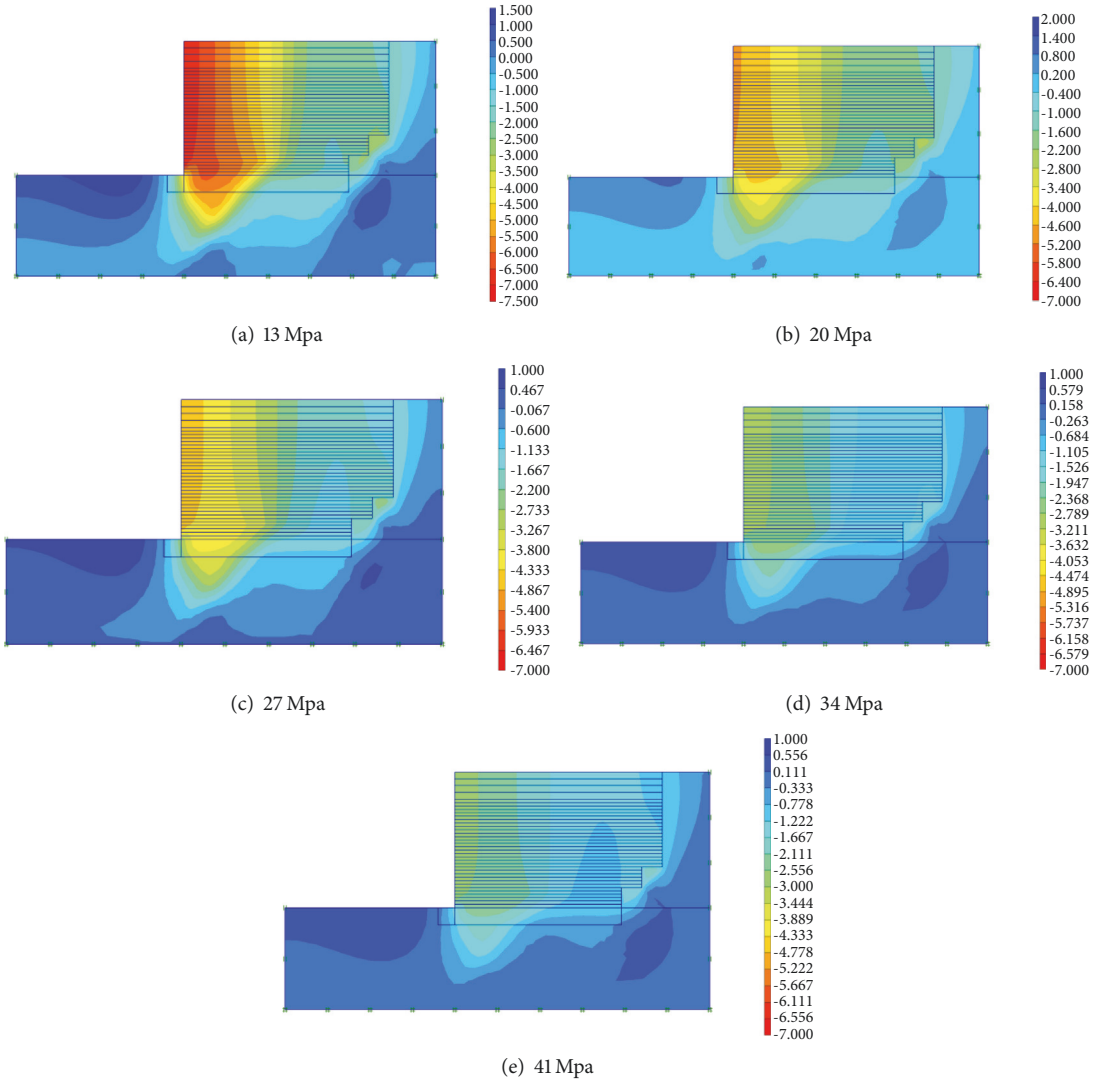

Figure 3: Influence of foundation soil on vertical deformation of the retaining wall.

smaller than other factors. In addition, according to the observation data of the field test, the function of the grid is mainly reflected on the fracture surface of the wall. Therefore, the layout of the geogrid needs to be combined with the fracture surface of the retaining wall.

3.3. The Influence of Fillers on the Deformation of the Retaining Wall. Three kinds of materials, lime soil, fly ash, and silty clay, are selected for finite element analysis; the effects of fillers on the horizontal and vertical deformation of the wall are shown in Figures 6 and 7.

It can be seen from Figure 5 that the maximum horizontal displacement of the wall is the largest when the filler is made of silty clay. The maximum displacement of lime soil and fly ash is reduced by 35% and 66%, respectively when they are used as fillers. When fly ash is used as filler, the deformation of the wall surface is composed of two forms of wall outward camber and arc-shaped external drum, and it can be clearly seen that the external drum appears at the height of 1.4 m. When lime soil is used as filler, the deformation type of the wall is the whole slippage; the wall is extroverted when the fly ash is used as a filler.

It can be seen from Figure 6 that the vertical deformation of retaining wall is the most serious when silty clay is used as filler, and it decreases rapidly with the retaining wall inward, which is easy to form uneven settlement, even potential safety hazard.

The fly ash has such a smaller density that the horizontal displacement of the wall is smaller and the effect is obvious, compared with the silty clay as a filler. This is mainly because the fly ash increases the shear strength of a larger range of soil in the reinforced backfill area, reducing the effect of backfill on the wall panels, enhancing the strength of the retaining wall, and reducing the horizontal displacement of the wall finally. The cohesive force of the lime soil is strong, which inhibits the deformation of the wall. By the comparison, fly ash and lime soil are both suitable as fillers for reinforced retaining wall.

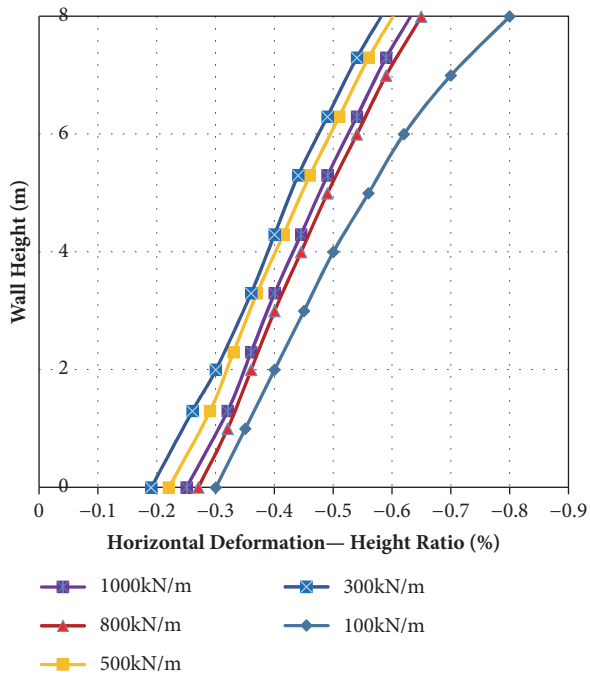

Figure 4: Influence of geogrid strength on horizontal deformation of the wall.

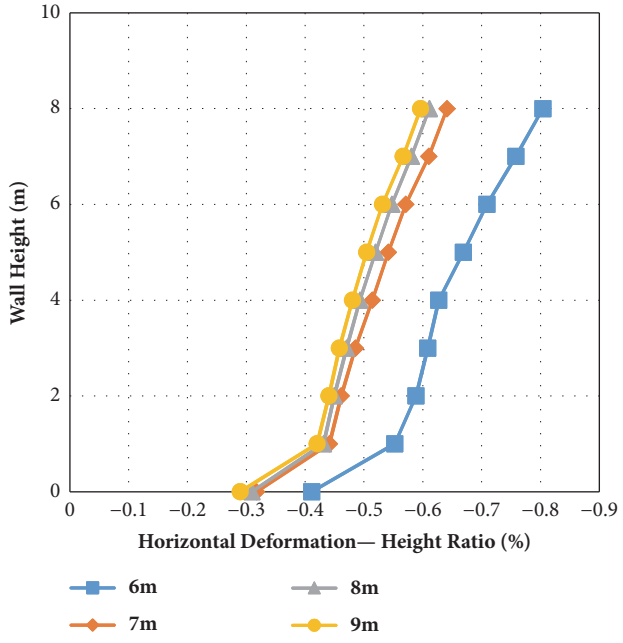

Figure 5: Influence of geogrid length on horizontal deformation of the wall.

4. Conclusion

The finite element model of reinforced soil retaining wall is divided into four parts: the soil packing unit, the reinforced material unit, the wall panel unit, and the contact surface unit. The reasonable constitutive relations of these four finite elements are selected and their corresponding element matrices are established. Taking the typical influencing factors as an example, a finite element deformation analysis model of reinforced soil retaining wall is established.

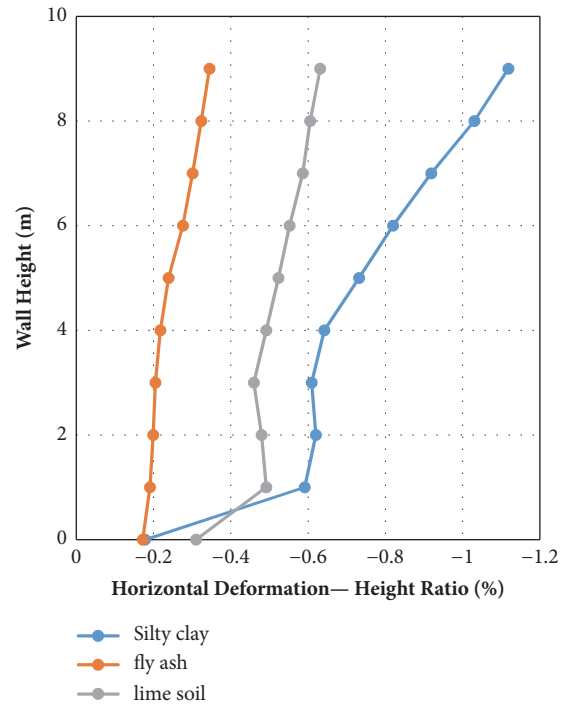

Figure 6: The effect of fillers on horizontal deformation of the wall.

Through the comparison of different elastic modulus of foundation soil displacement and horizontal wall settlement, foundation soil modulus of deformation of reinforced soil retaining wall is analyzed, the harm and the poor soil may cause,

By comparing the horizontal displacement and settlement of the wall when the foundation soil has different elastic modulus, the influence of the modulus of the foundation soil on the deformation of the reinforced soil retaining wall and the possible harm caused by the bad foundation soil are analyzed, which shows the importance of foundation treatment on the deformation and stability of the retaining wall.

The strength of geogrid has a certain impact on the vertical deformation of the retaining wall and a greater impact on the horizontal deformation, by comparing the influence of geogrid strength, length, and spacing on the deformation of reinforced soil retaining wall. The stability of retaining wall increases with the increasing of reinforcement length within a reasonable range, and the reinforcement length has little effect on the deformation of retaining wall beyond a certain threshold. The effect of continuous reduction of the reinforcement spacing on the horizontal deformation of the wall is not obvious similarly, when the spacing between stiffeners is reduced to a certain extent,

With the comparing of the influence of lime soil, fly ash, and silty clay filler on the deformation of retaining wall, the performance of lime soil filler is slightly better than that of fly ash; fly ash and lime soil are both suitable for filling the reinforced soil retaining wall, while silty clay is not suitable.

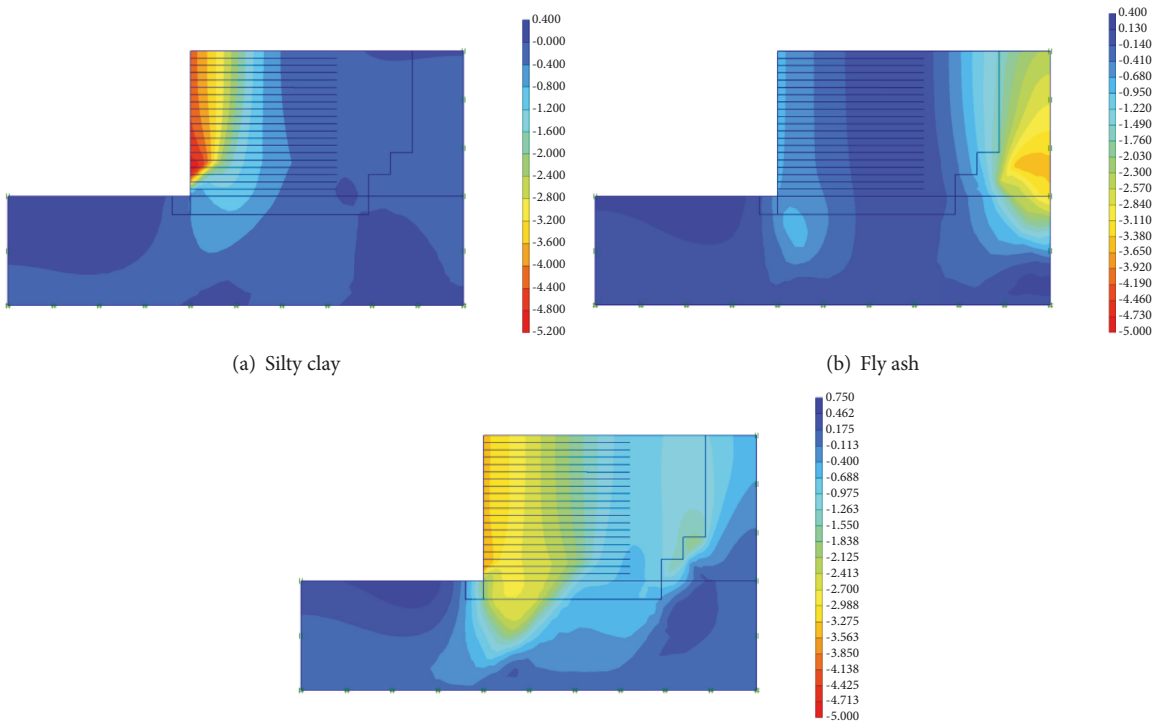

(a) Silty clay

(b) Fly ash

(c) Lime soil

Figure 7: The effect of filler on vertical deformation of retaining wall.

At the same time, the compaction of fillers and the mixing of lime soil will affect the properties of fillers and further affect the deformation and stability of the retaining wall. Therefore it is necessary to strictly control packing compaction and lime soil mixing.

Conflicts of Interest

The authors declare that there are no conflicts of interest regarding the publication of this paper.

Acknowledgments

This research was supported in part by the National Key Research and Development Program of China (no. 2016YFC0802208), the Natural Science Foundation of Shaanxi Province (no. 2017JQ5122), and the Fundamental Research Funds for the Central Universities of China (no. 300102218409 and no. 300102218521). The authors would like to thank Zhang Kewen for excellent technical support.

References

[1] G. Q. Yang, J. X. Ding, Q. Y. Zhou et al., "Field behavior of a geogrid reinforced soil retaining wall with a wrap-around facing," *Geotechnical Testing Journal*, vol. 33, no. 1, pp. 1–6, 2010.

[2] H. I. Ling, C. P. Cardany, L.-X. Sun, and H. Hashimoto, "Finite element study of a geosynthetic-reinforced soil retaining wall with concrete-block facing," *Geosynthetics International*, vol. 7, no. 3, pp. 163–188, 2000.

[3] Ö. Bilgin, "Failure mechanisms governing reinforcement length of geogrid reinforced soil retaining walls," *Engineering Structures*, vol. 31, no. 9, pp. 1967–1975, 2009.

[4] G. Q. Yang, X. L. Du, and Q. Y. Zhou, "Field tests on behaviors of geogrid-reinforced lime treated soil retaining walls," *Geotechnical Testing Journal*, vol. 32, no. 12, pp. 1904–1909, 2010.

[5] I. Mehdipour, M. Ghazavi, and R. Z. Moayed, "Numerical study on stability analysis of geocell reinforced slopes by considering the bending effect," *Geotextiles and Geomembranes*, vol. 37, pp. 23–34, 2013.

[6] C. Yoo and S.-B. Kim, "Performance of a two-tier geosynthetic reinforced segmental retaining wall under a surcharge load: Full-scale load test and 3D finite element analysis," *Geotextiles and Geomembranes*, vol. 26, no. 6, pp. 460–472, 2008.

[7] W. G. Clough and J. M. Duncan, "Finite element analyses of retaining wall behavior," *Asce Soil Mechanics & Foundation Division Journal*, vol. 97, no. 21, pp. 1657–1673, 1971.

[8] F. Zhang, "Field test research on geogrid reinforced earth high retaining wall," *Zhongguo Tiedao Kexue/China Railway Science*, vol. 29, no. 4, pp. 1–7, 2008.

[9] C. Jianfeng and Q. Hao, "Analysis of Deformation Relevance between Foundation and Flexible Facing for Geosynthetic-reinforced Soil Retaining Walls on Soft Clay," *Chinese Quarterly of Mechanics*, vol. 31, no. 3, pp. 425–429, 2010.

[10] I. Anastasopoulos, T. Georgarakos, V. Georgiannou, V. Drosos, and R. Kourkoulis, "Seismic performance of bar-mat reinforced-soil retaining wall: Shaking table testing versus numerical analysis with modified kinematic hardening constitutive model," *Soil Dynamics and Earthquake Engineering*, vol. 30, no. 10, pp. 1089–1105, 2010.

[11] Y. M. Mowafy and El-Sakhawy, "Parametric Study and Design Charts Based on Movement of Reinforced Earth Retaining Wall," *Information In Geo-Engineering*, pp. 553–561, 2010.

[12] Y. Shikou and R. Xuhua, "Mechanism and Stability Evaluation of Earth Slope Reinforced with Stone Columns," *Journal of China Three Gorges University*, vol. 33, no. 1, pp. 46–50, 2011.

[13] Y. Guanbao and Z. Zhen, "Influence of facing on mechanical behavior of reinforced retaining wall for embankment," *Rock and Soil Mechanics*, vol. 33, no. 3, pp. 881–886, 2012.

[14] H. H. Bui, J. K. Kodikara, A. Bouazza, A. Haque, and P. G. Ranjith, "A novel computational approach for large deformation and post-failure analyses of segmental retaining wall systems," *International Journal for Numerical and Analytical Methods in Geomechanics*, vol. 38, no. 13, pp. 1321–1340, 2014.

[15] A. Ouria, V. Toufigh, C. Desai, V. Toufigh, and H. Saadatmanesh, "Finite element analysis of a CFRP reinforced retaining wall," *Geomechanics and Engineering*, vol. 10, no. 6, pp. 757–774, 2016.

[16] K. Sukmak, J. Han, P. Sukmak, and S. Horpibulsuk, "Numerical parametric study on behavior of bearing reinforcement earth walls with different backfill material properties," *Geosynthetics International*, vol. 23, no. 6, pp. 435–451, 2016.

[17] W. Yankai, L. Jixing, and S. Yubin, "Dynamic Characteristic Analysis of Reinforced Earth Retaining Walls under Seismic Load," *China Earthquake Engineering Journal*, vol. 39, no. 3, pp. 475–480, 2017.

[18] M. Aghayarzadeh, "The effect of reinforced block rotation on face horizontal deformation of Geogrid reinforced soil retaining walls," *Journal of Clinical Psychopharmacology*, vol. 10, no. 2, pp. 96–104, 2012.

[19] S. L. Wen and H. B. La, "Analysis of engineering application about reinforced earth retaining wall," *Applied Mechanics and Materials*, vol. 353-354, pp. 585–588, 2013.

[20] F. M. Ezzein and R. J. Bathurst, "A new approach to evaluate soil-geosynthetic interaction using a novel pullout test apparatus and transparent granular soil," *Geotextiles and Geomembranes*, vol. 42, no. 3, pp. 246–255, 2014.

[21] S. M. B. Helwany, M. Budhu, and D. McCallen, "Seismic analysis of segmental retaining walls. I: Model verification," *Journal of Geotechnical and Geoenvironmental Engineering*, vol. 127, no. 9, pp. 741–749, 2001.

[22] B. Ram Rathan Lal and J. N. Mandal, "Experimental and finite element analysis of geocell reinforced fly ash retaining wall," in *Proceedings of the 26th International conference on Solid Waste Technology and Management*, pp. 403–413, Philadelphia, Pa, USA, March 2011.